Science World Journal Vol. 20(No 2) 2025 https://dx.doi.org/10.4314/swj.v20i2.32
www.scienceworldjournal.org
ISSN: 1597-6343 (Online), ISSN: 2756-391X (Print)
Published by Faculty of Science, Kaduna State University

Full Length Research Article

TURBULENT BOUNDARY LAYER FLOW IN THE PRESENCE OF CONSTANT PRESSURE GRADIENT AND THERMAL RADIATION

*[1]Yakubu M. Lawal, [1]Ayankop E. Andi, [2]Joseph K. Moses, [2]Abdullahi Aminu, [3]Joshua B. Hassan, [4]Wachin A.A.

[1]Department of Mathematical Sciences, Nigerian Defence Academy, Kaduna, Nigeria
[2]Department of Mathematical Sciences, Kaduna State University, Kaduna, Nigeria
[3]Department of Computer Science, Federal University Oye, Ekiti, Nigeria
[4]Department of mathematics, Air force Institute of Technology, Kaduna, Nigeria

*Corresponding Author Email Address: muntakayakubu@nda.edu.ng

ABSTRACT
This study investigates turbulent boundary layer flow under the influence of a constant pressure gradient and thermal radiation. The governing equations—continuity, momentum (a nonlinear differential equation), and energy—were solved using the He-Laplace method, which combines the Homotopy Perturbation Method with the Laplace Transform Technique. This approach yielded the velocity and temperature profiles of the flow. The effects of various fluid parameters were examined: the magnetic parameter(M), suction parameter (S), and pressure gradient (Ω) on velocity profiles; and the thermal radiation parameter (N), Eckert number(Ec), Prandtl number (Pr), and suction parameter (S) on temperature profiles. Corresponding graphs were plotted to illustrate these influences. The results indicate that an increase in the thermal radiation parameter raises the temperature field, while an increase in the magnetic parameter reduces the velocity field. A higher Prandtl number diminishes the temperature profile, and increasing the suction parameter reduces both velocity and temperature fields. Additionally, velocity increases with a greater pressure gradient, and a higher Eckert number enhances the temperature profile. These findings have practical implications in thermal processes across various engineering applications, such as in automotive systems, magnetohydrodynamic (MHD) power generators, and industrial operations like polymer extrusion and plastic film drainage.

Keywords: Turbulent, Boundary layer, thermal radiation, Pressure gradient

INTRODUCTION

In Physics and fluid mechanics, the boundary layer is the thin layer of fluid in the immediate vicinity of a bounding surface formed by the fluid flowing along the surface. The fluid's interaction with the wall induces a no-slip boundary condition (zero velocity at the wall). The flow velocity then monotonically increases above the surface until it returns to the bulk flow velocity. The thin layer consisting of fluid whose velocity has not yet returned to the bulk flow velocity is called the velocity boundary layer.

The standard formulation of the boundary layer equations is used and analytically solved until the point of flow separation for the unsteady state one dimensional turbulent boundary layer flow of an incompressible fluid over a flat plate under radiation and pressure gradient effects. The non-dimensional form of the corresponding equations with pressure gradient and thermal radiation are obtained. The resulting non-dimensional equations form a nonlinear partial differential equations, accompanied by sufficient boundary conditions. Such kinds of systems have been studied in literature using mostly numerical methods, since finding an analytical solution is very difficult, if at all possible. However, instead of using numerical method in order to solve this system of PDE's, one may choose a semi-analytical technique. The major advantage when using a semi-analytical technique instead of numerical is that a closed form approximate formula for the solution is obtained. This may lead to useful formula, even if they are approximation for quantities of physical interest. In addition, the implementation of semi-analytical techniques is highly facilitated nowadays by the used of symbolic computation software.

Approximate methods have been successfully applied in the past in order to study fluid mechanics problems. The most well-known approximate methods are perturbation techniques Dyke (1975). For recent applications of perturbation techniques to fluid mechanics problems, one may refer to Housiadas & Tanner (2006), Housiadas *et al*., (2015). Other approximate techniques have also been applied in the study of various physical problems, including boundary layer flows. The references of the present research are confined to few indicative papers of the last decade. It is worth mentioning that the differential transform method, combined with the method of steps, has been successfully applied for solving PDE's Rebenda & Samarda, 2015) as well as delayed DE's and systems, Rebenda & Samarda (2019).

A breakthrough for the approximate methods Liao's homotopy analysis method, (HAM), which was introduced Liao (1992). Since then, it has been extensively used for a variety of physical problems, such as beam problems, oscillation problems, wave propagation problems and of course, fluid mechanics problems. A thorough description of HAM can be found in Liao (2004) & (2011), where it is also shown how other approximate methods can be unified by HAM. The first papers where HAM was used for the study of boundary layer problems were Liao (1997) & (1999), where the Blasius and Falkner Skan equations was solved. Ever since, HAM has been successfully used, literally in hundreds of papers, for the study of boundary layer flows. In vast majority of the papers regarding boundary flow where HAM was used, the nonlinear equations under consideration were homogeneous with boundary conditions at ∞. There are, however, also papers of this kind where the solved nonlinear equations are nonhomogeneous, but in most cases, the nonhomogeneous term is a constant. Even less are papers of this kind, where the boundary conditions are not placed at ∞ but at some finite point.

Turbulent boundary layer is marked by mixing across several layers of it. The mixing is now on a macroscopic scale. Packets of fluid may be seen moving across. Thus, there is an exchange of mass, momentum and energy on a much bigger scale compared

to a laminar boundary layer. A turbulent boundary layer forms only at larger Reynolds number. The scale of mixing cannot be handled by molecular viscosity alone. Those calculating turbulent flow rely on what is called turbulence viscosity or Eddy viscosity, which has no exact expression. As a consequence of intense mixing a turbulent bound layer has a step gradient of velocity at the wall and therefore a large shear stress. In addition, heat transfer rates are also high.

Thermal radiation has also significant effects on the fluid flow, especially at high temperature with important engineering applications. Free convective laminar flow in the presence of radiation has been studied by Reptis & Toki (2009). Thermal radiation of an optically tin gray fluid has been studied in several incompressible flow configurations Reptis & Perdikis (2003). Other have studied radiation effects on flow past a stretching plate with temperature dependent viscosity Xenos (2013). The interaction of thermal radiation on a vertical oscillating plate and the effect of radiation on a moving vertical plate have been studied by Muthucumaraswamy (2006).

Although many studies exist on radiation effects on laminar incompressible flows, the study of MHD, compressible and turbulent boundary layer flow under the influence of thermal radiation and adverse pressure gradient has received little attention. The emission turbulence-radiation interaction in hypersonic boundary layer flow was studied by Duan *et al*., (2016). In this study, when emission is coupled to the flow, the temperature is drastically decreased in the turbulent layer. Liao (2004) used the basis ideas of the homotopy in topology to propose general analytical method of nonlinear problems. Namely, the so called Homotopy Analysis Method, (HAM) was proposed to obtain series solutions for nonlinear differential equations. Kafoussias & Xenos (2000) studied the effect of heat and mass transfer on the steady Reynolds averaged boundary layer equations and their boundary conditions were transformed in a suitable form for numerical solution by using the compressible version of the Falkner-Skan transformation. The resulting coupled and nonlinear system of partial differential equation was solved using the Keller's box method and a modified version of it.

The thermal radiation effects on unsteady free convective flow of a viscous incompressible flow past an infinite vertical oscillating plate with variable temperature and mass diffusion has been studied by Muthucumaraswamy (2006). The fluid considered here is a gray, absorbing-emitting radiation but a non-scattering medium. The plate temperature is raised linearly with respect to time and the concentration level near the plate is also raised linearly with respect to time. An exact solution to the dimensionless governing equations has been obtained by the Laplace transform method, when the plate is oscillating harmonically in its own plane. The effects of velocity, temperature and concentration are studied for different parameters like phase angle, radiation parameter, Schmidt number, thermal Grashof number, mass Grashof number and time are studied. It is observed that the velocity increases with decreasing phase angle. Mark *et al*., (2009) described the new high-resolution code for the direct simulation of incompressible boundary layers over a flat plate. The code can accommodate a wide range of pressure gradients, and general time dependent boundary conditions such as incoming wakes or wall forcing. The consistency orders of the advective and pressure-correction steps are different, but it is shown that the overall resolution is controlled by the higher-order advection steps. The formulation of boundary conditions to ensure global mass conservation in the presence of arbitrary forcing was carefully analyzed. Duan *et al*., (2011) conducted a direct numerical simulation to study the effects of emission turbulence-radiation interaction in hypersonic turbulent boundary layers, representative of the orion crew exploration vehicle at peak-heating condition during reentry. A non-dimensional governing parameter to measure the significance of emission turbulence radiation interaction is proposed, and the direct numerical simulation fields with and without emission. Both the uncoupled and coupled results show that there is no sizable interaction between turbulence and emission at the hypersonic environment under investigation. Xenos (2017) investigated the effect of radiation on the flow over a stretching plate of an optically thin gray, viscous and incompressible fluid is studied. The fluid viscosity is assumed to vary as an inverse linear function of the temperature. The partial differential equations (PDEs) and their boundary conditions, describing the problem under consideration, are dimensionalized and the numerical solution is obtained by using the finite volume discretization methodology which is suitable for fluid mechanics applications. The numerical results for the velocity and temperature profiles are shown for different dimensionless parameters entering the problem under consideration, such as the temperature parameter, θr, the radiation parameter, S, and the Prandtl number, Pr. The numerical results indicate a strong influence of these parameters on the non-dimensional velocity and temperature profiles in the boundary layer. Hughes & Brighton (1991) studied the steady, creeping and isothermal sedimentation of a rigid sphere in an incompressible viscoelastic fluid which follows the exponential Phan–Thien and Tanner constitutive equation is studied analytically. The solution of the governing equations is expanded as a regular perturbation series for small values of the Deborah number, and the resulting sequence of two-dimensional partial differential equations is solved analytically up to eighth order. Although the domain is unbounded, the solution is able to resolve features of the flow that cannot be revealed by a low-order theoretical analysis, such as very fine flow structures and a stress boundary layer close to the surface of the sphere. The calculation of the drag force exerted on the sphere by the fluid was done by developing two formulas. The first is based on the flow-field close to the sphere and the second is based on the far flow-field. Both formulas produce the same analytical expressions verifying the correctness and consistency of the series solution. At small Deborah numbers, a decrease of the drag force is predicted (i.e., an increase of the sedimentation velocity), followed by a significant drag enhancement at higher Deborah numbers. Investigation of the solution for the existence of a negative wake close to the rear stagnation point did not reveal such a phenomenon when physical constraints on the solutions were posed. On the contrary, a negative wake is predicted only as an artifact due to the loss of positive definiteness of the conformation tensor. It is also demonstrated that the effect of viscoelasticity is maximized in a region around the sphere with a radius which is about ten times the radius of the sphere. Last, it is shown that the fluid disturbances due to the viscoelasticity of the matrix fluid decay very slowly with the distance from the sphere, depending on the magnitude of the Deborah number. Streamlines, extra-stress and pressure contours as well as the extension of the polymer molecules are also presented and discussed. Nargund *et al*., (2017) investigated the compressible fluid flow in boundary layer region by Homotopy Analysis Method (HAM). Using Falkner-Skan Transformation, the governing partial differential equation were reduced into two nonlinear partial differential equations. These

Science World Journal Vol. 20(No 2) 2025 https://dx.doi.org/10.4314/swj.v20i2.32
www.scienceworldjournal.org
ISSN: 1597-6343 (Online), ISSN: 2756-391X (Print)
Published by Faculty of Science, Kaduna State University

equations were solved by Homotopy Analysis Method and the convergence of this, studied by using the Domb sykes plot. The effect of suction and injection were studied on the velocity and temperature distribution and were depicted in a graph. Xenos & Pop (2017) studied the combined effect of magnetic field thermal radiation and local suction on the steady turbulent compressible boundary layer flow with adverse pressure gradient numerically. The magnetic field was constant and applied transversely to the direction of the flow. The fluid was subjected to a localized suction and was considered as a radiative optically thin gray fluid. The Reynolds-averaged Boundary Layer equations with appropriate boundary conditions were transformed using the compressible Falkner-Skan transformation. Housiadas & Tanner (2018) studied the effect of steady shear flow on an infinitely long and freely rotating circular cylinder using asymptotic methods. The ambient fluid is assumed viscoelastic and modeled with the Oldroyd-B constitutive equation under isothermal and creeping flow conditions. The solution for all the dependent variables is expanded as an asymptotic power series with the small parameter being the Weissenberg number, Wi, which is defined as the product of the single relaxation time of the fluid times the externally imposed shear rate. The resulting sequence of equations is solved analytically up to the eighth order in the Weissenberg number, leading to a series solution, the accuracy and validity of which is shown to be linked to the loss of positive definiteness of the conformation tensor. The solution derived here is the first analytical result in the literature for viscoelastic fluids past a freely rotating cylinder. It reveals the slowdown of the rotation of the cylinder with respect to the Newtonian case, as previously found for the same type of flow past a rigid sphere. It is also seen that the first correction to the velocity profile is of second order in Wi, while that for the pressure is of first order. This contrasts with the solution for the viscoelastic flow past a sphere for which the correction for both the velocity and pressure profiles are of first order in Wi. The analytical solution also shows that the region of closed streamlines around the cylinder is enlarged compared to the Newtonian case. Last, it is seen that the up-and-down and fore-and-aft symmetries of the streamlines and the vorticity contours, observed for Newtonian fluids, break in the viscoelastic case. Rabenda & Smarda (2016), described propose a semi-analytical technique convenient for numerical approximation of solutions of the initial value problem for p-dimensional delayed and neutral differential systems with constant, proportional and time varying delays. The algorithm is based on combination of the method of steps and the differential transformation. Convergence analysis of the presented method is given as well. Applicability of the presented approach is demonstrated in two examples. A system of pantograph type differential equations and a system of neutral functional differential equations with three types of delays are considered. The accuracy of the results is compared to those obtained by the Laplace decomposition algorithm, the residual power series method and Matlab package DDENSD. A comparison of computing time is presented, too, showing reliability and efficiency of the proposed technique. Sharma *et al*., (2019) used on analytical technique known as homotopy analysis method to acquire solutions for magnetohydrodynamic 3-D motion of a viscous nanofluid over a saturated porous medium with a heat source and thermal radiation. The governing nonlinear partial differential equations are changed to ordinary differential equations, employing appropriate transformations. Validation of the present result is done with the help of error analysis for flow and temperature. The influences of pertinent parameters on momentum, energy and Nusselt number are studied and discussed. The major findings are velocity of the nanofluid is affected by the nano particles volume fraction and the thickness of the thermal boundary layer becomes thinner and thinner subject to sink, whereas the effect is revered in case of the source.

In these studies, however, the fluid flows considered were compressible. But it is a known fact that most fluids used in Engineering and hydraulics are mainly incompressible.

Years later, Xenos *et al*., (2020) studied the steady state, two dimensional, laminar, boundary layer flow of an incompressible fluid over a flat plate under radiation and pressure gradient effects, and solution was obtained using Homotopy Analysis Method; an analytical technique for the first time.

Most existing studies focus on either turbulent boundary layers under zero or varying pressure gradients, or radiative heat transfer in laminar or simplified turbulent flows. However, this work fills the gap by investigating fully turbulent boundary layers under a constant pressure gradient with thermal radiation. Turbulent boundary layer flows are fundamental to many engineering systems, including aerospace, energy, and environmental applications. When these flows occur under a **constant pressure gradient** and are influenced by **thermal radiation**, the complexity increases significantly. Understanding this interaction is crucial for; improving **thermal management** in high-speed vehicles and reactors, Enhancing **predictive models** for heat transfer in turbulent regimes and Designing more efficient **cooling systems** in industrial processes.

MATERIALS AND METHODS

We consider an unsteady, one-dimensional turbulent flow of an incompressible fluid in the boundary layer that forms over a flat plate parallel to the free stream velocity, $U_\infty$is considered. In a Cartesian coordinate system (x, y), the surface is located at $y = 0, 0 \leq x \leq L$, as shown in Figure 1 below.

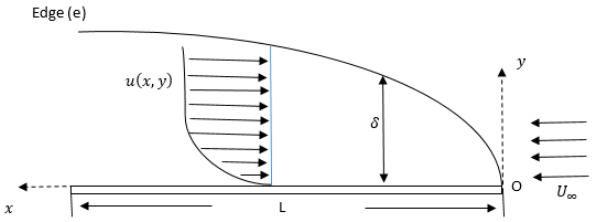

Figure 1: Flow Configuration and Coordinate System

The following assumptions have been made,

- Unsteady state
- One-dimensional flow
- The suction is assumed
- The plate is infinite and the fluid motion is unsteady, so all the flow variables depend on y and t only
- The x-axis is normal to the plate in the direction of the flow
- The y-axis is taken along the plate in the vertical direction

The governing equations for the boundary layer simplifications consist of the continuity equation

$$\frac{\partial u}{\partial y} = 0 \quad (1)$$

The momentum equation,

$$\rho\left(\frac{\partial u}{\partial t} + v\frac{\partial u}{\partial y}\right) = -\frac{dp}{dx} + \vartheta\frac{\partial^2 u}{\partial y^2} - \sigma B_0^2 u - \frac{\mu}{k}u \quad (2)$$

And the energy equation,

$$\rho C_p\left(\frac{\partial T}{\partial t} + v\frac{\partial u}{\partial y}\right) = K\frac{\partial^2 T}{\partial y^2} + \mu\left(\frac{\partial u}{\partial y}\right)^2 - \frac{\partial q_r}{\partial y} \quad (3)$$

The initial and boundary conditions are

$u(y,t) = u_0 e^{-yh}, T = T_0 + (T_w - T_\infty)e^{-yh}$ at $t = 0$, for $0 \le y \ge h$

$u(y,t) = u_0, T(y,t) = T_0 + (T_w - T_\infty)$ at $y = h$, for $t > 0$ (4)

Where $u\ and\ v$ are the velocity components, T is the temperature, p is the pressure, ρ is the density, ϑ is the kinematic viscosity, μ is the dynamic viscosity, C_p is the specific temperature of the fluid under constant pressure, k is the coefficient of thermal conductivity, σ is the Stefan Boltzmann constant, $\frac{\partial q_r}{\partial y}$ is the local radiant absorption, T_0 is the temperature of the fluid, T_w is the temperature of the flat plate, T_∞ is the ambient temperature at the boundary layer, and δ is the boundary layer thickness.

Equations (1), (2), and (3) with the boundary conditions (4) will be solved using He-Laplace Techniques (Perturbation Method), to obtain velocity, pressure, and energy for the boundary layer flow, under consideration.

To the non-dimensional equations (1) – (4), the following dimensionless parameters are introduced [29]

$$u^* = \frac{u}{u_0}, \quad P^* = \frac{p}{\mu u_0^2}, \quad t^* = \frac{tu_0^2}{\vartheta}, \quad M^2 = \frac{\sigma B_0^2 \vartheta}{\rho u_0^2}, \quad y^* = \frac{yv_0}{\vartheta},$$

$$x^* = \frac{x}{u_0}, \quad S = \frac{v_0}{u_0}, \quad v^* = \frac{v}{u_0}, \quad D_a = \frac{kv_0^2}{\vartheta^2}, \quad \theta = \frac{T - T_0}{T_w - T_\infty}, \quad P_r = \frac{\rho v_0^2}{\vartheta^2}, \quad N = \frac{4\alpha^2}{\rho C_p v_0^2},$$

$$p_r = \frac{\rho C_p}{k}, \quad \frac{\partial q_r}{\partial y} = 4\alpha^2(T_0 - T), \quad E_c = \frac{\vartheta U_0^2}{C_p(T_w - T_\infty)}, \quad h = \frac{u_0}{\vartheta} \quad (5)$$

Substituting equation (5) into equations (1) – (4) and by dropping the asterisks, we have the following

$$\frac{\partial u}{\partial t} - s\frac{\partial u}{\partial y} = -\frac{\partial p}{\partial x} + \frac{\partial^2 u}{\partial y^2} - \left(M^2 + \frac{1}{Da}\right)u \quad (6)$$

$$\frac{\partial \theta}{\partial t} - s\frac{\partial \theta}{\partial y} = \frac{1}{p_r}\frac{\partial^2 \theta}{\partial y^2} + E_c\left(\frac{\partial u}{\partial y}\right)^2 + N\theta \quad (7)$$

The Initial and Boundary Conditions:

$u(y,t) = e^{-y}, \theta(y,t) = e^{-y}\ at\ t = 0\ for\ 0 \le y \ge 1$

$u(y,t) = 1, \theta(y,t) = 1\ at\ y = 1\ for\ t > 0$ (8)

Solution of the Problem

In this section, we employed the He – Laplace method to solve equations (6) and (7) subject to equation (8)

Taking the Laplace transform of (6); gives

$$\mathcal{L}\left\{\frac{\partial u}{\partial t}\right\} - \mathcal{L}\left\{s\frac{\partial u}{\partial t}\right\} = \mathcal{L}\{\Omega\} + \mathcal{L}\left\{\frac{\partial^2 u}{\partial y^2}\right\} - \mathcal{L}\{L_1 u\} \quad (9)$$

Where $-\frac{\partial p}{\partial x} = \Omega, \quad L_1 = \left(M^2 + \frac{1}{Da}\right)$ (10)

But $\mathcal{L}\left\{\frac{\partial u}{\partial t}\right\} = s\mathcal{L}\{u(y,t)\} - u(y,0)$

Thus, $s\mathcal{L}\{u(y,t)\} - u(y,0) - \mathcal{L}\left\{s\frac{\partial u}{\partial t}\right\} = \mathcal{L}\{\Omega\} + \mathcal{L}\left\{\frac{\partial^2 u}{\partial y^2}\right\} - \mathcal{L}\{L_1 u\}$ (11)

Applying the initial condition on eqn. (11), one obtains,

$$s\mathcal{L}\{u(y,t)\} - e^{-y} - \mathcal{L}\left\{s\frac{\partial u}{\partial t}\right\} = \mathcal{L}\{\Omega\} + \mathcal{L}\left\{\frac{\partial^2 u}{\partial y^2}\right\} - \mathcal{L}\{L_1 u\}$$

Or,

$$s\mathcal{L}\{u(y,t)\} = e^{-y} + \mathcal{L}\left\{s\frac{\partial u}{\partial t}\right\} + \mathcal{L}\{\Omega\} + \mathcal{L}\left\{\frac{\partial^2 u}{\partial y^2}\right\} - \mathcal{L}\{L_1 u\} \quad (12)$$

Therefore, $\mathcal{L}\{u(y,t)\} = \frac{e^{-y}}{s} + \frac{1}{s}\mathcal{L}\{\Omega\} + \frac{1}{s}\left[\mathcal{L}\left\{\frac{\partial^2 u}{\partial y^2}\right\} + s\mathcal{L}\left\{\frac{\partial u}{\partial t}\right\} - L_1\mathcal{L}\{u\}\right]$ (13)

Taking the Laplace inverse of (3.34), we have,

$$\mathcal{L}^{-1}\mathcal{L}\{u(y,t)\} = \mathcal{L}^{-1}\left\{\frac{e^{-y}}{s}\right\} + \mathcal{L}^{-1}\left\{\frac{1}{s}\mathcal{L}\{\Omega\}\right\} + \mathcal{L}^{-1}\left[\frac{1}{s}\left[\mathcal{L}\left\{\frac{\partial^2 u}{\partial y^2}\right\} + s\mathcal{L}\left\{\frac{\partial u}{\partial t}\right\} - L_1\mathcal{L}\{u\}\right]\right]$$

Science World Journal Vol. 20(No 2) 2025 https://dx.doi.org/10.4314/swj.v20i2.32
www.scienceworldjournal.org
ISSN: 1597-6343 (Online), ISSN: 2756-391X (Print)
Published by Faculty of Science, Kaduna State University

Or,

$$u(y,t) = \Omega + e^{-y} + \mathcal{L}^{-1}\left[\frac{1}{s}\left[\mathcal{L}\left\{\frac{\partial^2 u}{\partial y^2}\right\} + s\mathcal{L}\left\{\frac{\partial u}{\partial t}\right\} - L_1\mathcal{L}\{u\}\right]\right] \quad (14)$$

Applying the Homotopy Perturbation techniques, (14) yields.

$$\sum_{n=0}^{\infty} p^n u_n(y,t) = \Omega + e^{-y} + p\left[\mathcal{L}^{-1}\left[\frac{1}{s}\left[\mathcal{L}\left\{\frac{\partial^2 u}{\partial y^2}\right\} + s\mathcal{L}\left\{\frac{\partial u}{\partial t}\right\} - L_1\mathcal{L}\{u\}\right]\right]\right] \quad (15)$$

Comparing the coefficients of the like powers of $'p'$ on both sides of $eqn.(15)$, the following approximations are obtained;

$$p^0: u_0(y,t) = \Omega + e^{-y} \quad (16)$$

$$p^1: u_1(y,t) = \mathcal{L}^{-1}\left[\frac{1}{s}\left[\mathcal{L}\left\{\frac{\partial^2 u_0}{\partial y^2}\right\} + s\mathcal{L}\left\{\frac{\partial u_0}{\partial t}\right\} - L_1\mathcal{L}\{u_0\}\right]\right]$$

$$= \mathcal{L}^{-1}\left[\frac{1}{s}[\mathcal{L}\{e^{-y}\} + s\mathcal{L}\{-e^{-y}\} - L_1\mathcal{L}\{\Omega + e^{-y}\}]\right]$$

$$= \mathcal{L}^{-1}\left[\frac{e^{-y}}{s^2} - \frac{se^{-y}}{s^2} - \frac{1}{s^2}(\Omega + e^{-y})\right]$$

$$= \mathcal{L}^{-1}\left[\left(\frac{e^{-y}}{s^2}\right) - s\left(\frac{e^{-y}}{s^2}\right) - \frac{L_1\Omega}{s^2} - \frac{L_1 e^{-y}}{s^2}\right]$$

$$u_1(y,t) = (e^{-y} - se^{-y} - L_1\Omega - L_1e^{-y})t \quad (17)$$

$$p^2: u_2(y,t) = \mathcal{L}^{-1}\left[\frac{1}{s}\left[\mathcal{L}\left\{\frac{\partial^2 u_1}{\partial y^2}\right\} + s\mathcal{L}\left\{\frac{\partial u_1}{\partial t}\right\} - L_1\mathcal{L}\{u_0\}\right]\right]$$

$$= \mathcal{L}^{-1}\left[\frac{1}{s}\{\mathcal{L}(e^{-y} - se^{-y} - L_1e^{-y})t\} + s\mathcal{L}\{(se^{-y} + L_1e^{-y} - e^{-y})t\} - L_1\mathcal{L}\{(e^{-y} - se^{-y} - L_1\Omega - L_1e^{-y})t\}\right]$$

$$= \mathcal{L}^{-1}\left[\left(\frac{e^{-y} - se^{-y} - L_1e^{-y}}{s^3}\right) + \left(\frac{s^2e^{-y} + sL_1e^{-y} - se^{-y}}{s^3}\right) - L_1\left\{\left(\frac{e^{-y} - se^{-y} - L_1\Omega - L_1e^{-y}}{s^3}\right)\right\}\right]$$

$$= (e^{-y} - se^{-y} - L_1e^{-y})\frac{t^2}{2} + (s^2e^{-y} + sL_1e^{-y} - se^{-y})\frac{t^2}{2} - (L_1e^{-y} - sL_1e^{-y} - L_1^2\Omega - L_1^2e^{-y})\frac{t^2}{2!}$$

$$u_2(y,t) = (s^2e^{-y} - 2se^{-y} + 2L_1se^{-y} - 2L_1e^{-y} - L_1^2\Omega - L_1^2e^{-y} - e^{-y})\frac{t^2}{2} \quad (18)$$

$$p^3: u_3(y,t) = \mathcal{L}^{-1}\left[\frac{1}{s}\left[\mathcal{L}\left\{\frac{\partial^2 u_2}{\partial y^2}\right\} + s\mathcal{L}\left\{\frac{\partial u_2}{\partial t}\right\} - L_1\mathcal{L}\{u_2\}\right]\right]$$

$$= \mathcal{L}^{-1}\left[\frac{1}{s}\left\{\mathcal{L}(s^2e^{-y} - 2se^{-y} + 2L_1se^{-y} - 2L_1e^{-y} - L_1^2e^{-y} - e^{-y})\frac{t^2}{2!}\right\} + s\mathcal{L}\left\{(-s^2e^{-y} + 2se^{-y} - 2L_1se^{-y} + 2L_1e^{-y} + L_1^2e^{-y} + e^{-y})\frac{t^2}{2!}\right\} - L_1\mathcal{L}\left\{(s^2e^{-y} - 2se^{-y} + 2L_1se^{-y} - 2L_1e^{-y} - L_1^2\Omega - L_1^2e^{-y} - e^{-y})\frac{t^2}{2!}\right\}\right]$$

$$= \mathcal{L}^{-1}\left[\frac{1}{s^4}(s^2e^{-y} - 2se^{-y} + 2L_1se^{-y} - 2L_1e^{-y} - L_1^2e^{-y} - e^{-y}) + \frac{1}{s^4}(-s^2e^{-y} - 2s^2e^{-y} - 2L_1s^2e^{-y} + 2L_1se^{-y} + L_1^2se^{-y} + se^{-y}) - \frac{1}{s^4}(s^2L_1e^{-y} - 2sL_1e^{-y} + 2L_1^2se^{-y} - 2L_1^2e^{-y} - L_1^3\Omega - L_1^3e^{-y} - L_1e^{-y})\right]$$

$$u_3(y,t) = (-s^3e^{-y} - 3L_1s^2e^{-y} - s^2e^{-y} - L_1^2se^{-y} + 6L_1se^{-y} - se^{-y} + L_1^3e^{-y} + L_1^3\Omega + L_1^2e^{-y} - L_1e^{-y} - e^{-y})\frac{t^3}{3!} \quad (19)$$

Therefore, the solution of $eqn.(15)$ is obtained by adding together $eqns.(16) - (20)$, i.e,

$$u(y,t) = u_0(y,t) + u_1(y,t) + u_2(y,t) + u_3(y,t) + \cdots \quad (20)$$

Thus, $u(y,t) = (\Omega + e^{-y}) + (e^{-y} - se^{-y} - L_1\Omega - L_1e^{-y})t + (s^2e^{-y} - 2se^{-y} + 2L_1se^{-y} - 2L_1e^{-y} - L_1^2\Omega - L_1^2e^{-y} - e^{-y})\frac{t^2}{2!} + (-s^3e^{-y} - 3L_1s^2e^{-y} - s^2e^{-y} - L_1^2se^{-y} + 6L_1se^{-y} - se^{-y} + L_1^3e^{-y} + L_1^3\Omega + L_1^2e^{-y} - L_1e^{-y} - e^{-y})\frac{t^3}{3!} + \cdots \quad (21)$

Equation (21) gives the solution to the velocity equation (6).

Now, taking the Laplace transform of $eqn.(7)$, one obtains,

$$\mathcal{L}\left[\frac{\partial\theta}{\partial t}\right] - \mathcal{L}\left[s\frac{\partial\theta}{\partial y}\right] = \mathcal{L}\left[\frac{1}{p_r}\frac{\partial^2\theta}{\partial y^2}\right] + \mathcal{L}\left[E_c\left(\frac{\partial u}{\partial y}\right)^2\right] + \mathcal{L}[N\theta] \quad (22)$$

But $\mathcal{L}\left[\frac{\partial\theta}{\partial t}\right] = s\mathcal{L}[\theta(y,t)] - \theta(y,0)$,

Thus, equation (22) becomes

$$s\mathcal{L}[\theta(y,t)] - \theta(y,0) - \mathcal{L}\left[s\frac{\partial\theta}{\partial y}\right] = \mathcal{L}\left[\frac{1}{p_r}\frac{\partial^2\theta}{\partial y^2}\right] + \mathcal{L}\left[E_c\left(\frac{\partial u}{\partial y}\right)^2\right] + N\mathcal{L}[\theta]$$

Or,

$$s\mathcal{L}[\theta(y,t)] - e^{-y} = \frac{1}{p_r}\mathcal{L}\left[\frac{\partial^2\theta}{\partial y^2}\right] + E_c\mathcal{L}\left[\left(\frac{\partial u}{\partial y}\right)^2\right] + s\mathcal{L}\left[\frac{\partial\theta}{\partial y}\right] + N\mathcal{L}[\theta] \quad (23)$$

Further simplification yields;

$$\mathcal{L}[\theta(y,t)] = \frac{e^{-y}}{s} + \frac{1}{s}\left\{\frac{1}{p_r}\mathcal{L}\left[\frac{\partial^2\theta}{\partial y^2}\right] + s\mathcal{L}\left[\frac{\partial\theta}{\partial y}\right] + N\mathcal{L}[\theta] + E_c\mathcal{L}\left[\left(\frac{\partial u}{\partial y}\right)^2\right]\right\} \quad (24)$$

Taking the inverse Laplace transform of (24), we have;

$$\mathcal{L}^{-1}\{\mathcal{L}[\theta(y,t)]\} = \mathcal{L}^{-1}\left\{\frac{e^{-y}}{s} + \frac{1}{s}\left\{\frac{1}{p_r}\mathcal{L}\left[\frac{\partial^2\theta}{\partial y^2}\right] + s\mathcal{L}\left[\frac{\partial\theta}{\partial y}\right] + N\mathcal{L}[\theta] + E_c\mathcal{L}\left[\left(\frac{\partial u}{\partial y}\right)^2\right]\right\}\right\}$$

Or,

$$\theta(y,t) = e^{-y} + \mathcal{L}^{-1}\left\{\frac{1}{s}\left\{\frac{1}{p_r}\mathcal{L}\left[\frac{\partial^2\theta}{\partial y^2}\right] + s\mathcal{L}\left[\frac{\partial\theta}{\partial y}\right] + N\mathcal{L}[\theta] + E_c\mathcal{L}\left[\left(\frac{\partial u}{\partial y}\right)^2\right]\right\}\right\} \quad (25)$$

Applying the Homotopy Perturbation method to (25), we get,

$$\sum_{n=0}^{\infty} p^n\,\theta_n(y,t) = e^{-y} + p\left[\mathcal{L}^{-1}\left[\frac{1}{s}\left[\frac{1}{p_r}\mathcal{L}\left[\frac{\partial^2\theta}{\partial y^2}\right] + s\mathcal{L}\left[\frac{\partial\theta}{\partial y}\right] + N\mathcal{L}[\theta] + E_c\mathcal{L}[H_n(u)]\right]\right]\right] \quad (26)$$

Where $H_n(u)$ is the He's polynomial for the non-linear term $\left(\frac{\partial u}{\partial y}\right)^2$ which are:

$H_0(u) = (u_0')^2$
$H_1(u) = 2u_0'u_1'$
$H_2(u) = 2u_0'u_2' + (u_1')^2$
$H_2(u) = 2u_1'u_2'$, ...

Now comparing like powers of p on both sides of $eqn.(26)$ and equating their coefficient gives;

p^0: $\theta_0(y,t) = e^{-y}$ (27)

$$p^1\text{: } \theta_1(y,t) = \mathcal{L}^{-1}\left\{\frac{1}{s}\left\{\frac{1}{p_r}\mathcal{L}\left[\frac{\partial^2\theta_0}{\partial y^2}\right] + s\mathcal{L}\left[\frac{\partial\theta_0}{\partial y}\right] + N\mathcal{L}[\theta_0] + E_c\mathcal{L}[H_0(u)]\right\}\right\} \quad (28)$$

And, $u_0 = \Omega + e^{-y}$, from $eqn.(3.37)$
Which implies,
$u_0' = -e^{-y}$,
$(u_0')^2 = e^{-2y}$,
$\theta_0 = e^{-y}$, $from\ eqn.(27)$
Which implies,
$\theta_0' = -e^{-y}$,
$\theta_0'' = e^{-y}$.
Thus,

$$\theta_1(y,t) = \mathcal{L}^{-1}\left\{\frac{1}{s}\left\{\frac{1}{p_r}\mathcal{L}[e^{-2y}] + s\mathcal{L}[-e^{-y}] + N\mathcal{L}[e^{-y}] + E_c\mathcal{L}[e^{-2y}]\right\}\right\}$$

Or,

$$\theta_1(y,t) = \mathcal{L}^{-1}\left\{\frac{1}{s}\left\{\frac{e^{-2y}}{sp_r} - \frac{s}{s}e^{-y} + \frac{N}{s}e^{-y} + \frac{E_c}{s}e^{-2y}\right\}\right\}$$

Simplification yields,

$$\theta_1(y,t) = \mathcal{L}^{-1}\left\{\frac{1}{s^2}\left[\frac{e^{-2y}}{p_r} - se^{-y} + Ne^{-y} + E_ce^{-2y}\right]\right\}$$

Hence, $\theta_1(y,t) = \left(\frac{e^{-2y}}{p_r} - se^{-y} + Ne^{-y} + E_ce^{-2y}\right)t$ (29)

$$p^2\text{: } \theta_2(y,t) = \mathcal{L}^{-1}\left\{\frac{1}{s}\left\{\frac{1}{p_r}\mathcal{L}\left[\frac{\partial^2\theta_1}{\partial y^2}\right] + s\mathcal{L}\left[\frac{\partial\theta_1}{\partial y}\right] + N\mathcal{L}[\theta_1] + E_c\mathcal{L}[H_2(u)]\right\}\right\} \quad (30)$$

Since, $H_1(u) = 2u_0'u_1$
Thus, $H_1(u) = 2(-e^{-y})[(e^{-y} - se^{-y} - L_1\Omega - L_1e^{-y})t]$, from $eqn.(17)$.

$$= 2[(-e^{-2y} + se^{-2y} + L_1\Omega e^{-y} + L_1e^{-2y})]$$
$$= (2se^{-2y} + L_1e^{-2y} - e^{-2y} + L_1\Omega e^{-y})t \quad (31)$$

$eqn.(3.50)$,

$$\theta_1' = \left[\left(\frac{-2e^{-2y}}{p_r} + se^{-y} - Ne^{-y} - 2E_ce^{-2y}\right)t\right] \quad (32)$$

$$\theta_1'' = \left[\left(\frac{4e^{-2y}}{p_r} - se^{-y} + Ne^{-y} + 4E_ce^{-2y}\right)t\right] \quad (33)$$

Thus,

Science World Journal Vol. 20(No 2) 2025 https://dx.doi.org/10.4314/swj.v20i2.32
www.scienceworldjournal.org
ISSN: 1597-6343 (Online), ISSN: 2756-391X (Print)
Published by Faculty of Science, Kaduna State University

$$\theta_2(y,t) = \mathcal{L}^{-1}\left\{\frac{1}{s}\left\{\frac{1}{p_r}\mathcal{L}\left[\left(\frac{4e^{-2y}}{p_r} - se^{-y} + Ne^{-y} + 4E_c e^{-2y}\right)t\right] + s\mathcal{L}\left[\left(\frac{-2e^{-2y}}{p_r} + se^{-y} - Ne^{-y} - 2E_c e^{-2y}\right)t\right] + N\mathcal{L}\left[\left(\frac{-2e^{-2y}}{p_r} + se^{-y} - Ne^{-y} - 2E_c e^{-2y}\right)t\right] + E_c\mathcal{L}[(2se^{-2y} + L_1 e^{-2y} - e^{-2y} + L_1\Omega e^{-y})t]\right\}\right\}$$

Or,

$$\theta_2(y,t) = \mathcal{L}^{-1}\left\{\frac{1}{s^3}\left[\frac{4e^{-2y}}{p_r^2} - \frac{se^{-y}}{p_r} + \frac{Ne^{-y}}{p_r} + \frac{4E_c e^{-2y}}{p_r} - \frac{2se^{-2y}}{p_r} + s^2e^{-y} - Nse^{-y} - 2E_c se^{-2y} - \frac{2Ne^{-2y}}{p_r} + Nse^{-y} - N^2e^{-y} - 2E_c Ne^{-2y} + 2E_c se^{-2y} + E_c L_1 e^{-2y} - E_c e^{-2y} + E_c L_1\Omega e^{-y}\right]\right\} \quad (34)$$

Further simplification yields,

$$\theta_2(y,t) = \left(\frac{4e^{-2y}}{p_r^2} - \frac{se^{-y}}{p_r} + \frac{Ne^{-y}}{p_r} + \frac{4E_c e^{-2y}}{p_r} - \frac{2se^{-2y}}{p_r} + s^2e^{-y} - \frac{2Ne^{-2y}}{p_r} - N^2e^{-y} - 2E_c Ne^{-2y} + E_c L_1 e^{-2y} - E_c e^{-2y} + E_c L_1\Omega e^{-y}\right)\frac{t^2}{2!} \quad (35)$$

$$p^3\colon \theta_3(y,t) = \mathcal{L}^{-1}\left\{\frac{1}{s}\left\{\frac{1}{p_r}\mathcal{L}\left[\frac{\partial^2\theta_2}{\partial y^2}\right] + s\mathcal{L}\left[\frac{\partial\theta_2}{\partial y}\right] + N\mathcal{L}[\theta_2] + E_c\mathcal{L}[H_2(u)]\right\}\right\}$$

Since, $H_2 = 2u_0'u_2' + (u_1')^2$
Where, $u_0 = \Omega + e^{-y}$, $eqn.(16)$
$u_0' = -e^{-y}$
$u_2 = (s^2e^{-y} - 2se^{-y} + 2L_1e^{-y} - 2L_1e^{-y} - L_1^2\Omega - L_1^2e^{-y} - e^{-y})\frac{t^2}{2}$, $eqn.(18)$
Thus, $u_2' = (-s^2e^{-y} + 2se^{-y} - 2L_1e^{-y} + 2L_1e^{-y} + L_1^2e^{-y} + e^{-y})\frac{t^2}{2}$
And, $2u_0'u_2' = 2(-e^{-y})\left[(-s^2e^{-y} + 2se^{-y} - 2L_1e^{-y} + 2L_1e^{-y} + L_1^2\Omega + L_1^2e^{-y} + e^{-y})\frac{t^2}{2}\right]$
Or,

$$2u_0'u_2' = (2s^2e^{-2y} - 4se^{-2y} + 2L_1e^{-y} - 4L_1e^{-2y} - 2L_1^2e^{-2y} - 4e^{-2y})\frac{t^2}{2} \quad (36)$$

$u_1 = (e^{-y} - se^{-y} - L_1\Omega - L_1e^{-y})t$, $eqn.(17)$
Thus,
$u_1' = (-e^{-y} + se^{-y} + L_1e^{-y})t$
And, $(u_1')^2 = [(-e^{-y} + se^{-y} + L_1e^{-y})t][(-e^{-y} + se^{-y} + L_1e^{-y})t]$
Or,

$$(u_1')^2 = (e^{-2y} - se^{-2y} - L_1e^{-2y} - se^{-2y} + s^2e^{-2y} + L_1se^{-2y} - L_1e^{-2y} + L_1se^{-2y} + L_1^2e^{-2y})t^2$$

Further simplification yields,

$$(u_1')^2 = (e^{-2y} - 2se^{-2y} - 2L_1e^{-2y} + s^2e^{-2y} + 2L_1se^{-2y} + L_1^2e^{-2y})t^2 \quad (37)$$

Hence,

$$H_2 = 2u_0'u_2' + (u_1^1)^2 = (4s^2e^{-2y} - 8se^{-2y} + 2L_1e^{-y} - 8L_1e^{-2y} + 4L_1se^{-2y} - 4e^{-2y})\frac{t^2}{2} \quad (38)$$

And,

$$\theta_2' = \left(\frac{-8e^{-2y}}{p_r^2} - \frac{se^{-y}}{p_r} - \frac{Ne^{-y}}{p_r} - \frac{8E_c e^{-2y}}{p_r} + \frac{4se^{-2y}}{p_r} - s^2e^{-y} + \frac{4Ne^{-2y}}{p_r} + N^2e^{-y} + 4E_c Ne^{-2y} - 2E_c L_1e^{-2y} + 2E_c e^{-2y} - E_c L_1\Omega e^{-y}\right)\frac{t^2}{2} \quad (39)$$

$$\theta_2'' = \left(\frac{16e^{-2y}}{p_r^2} - \frac{se^{-y}}{p_r} + \frac{Ne^{-y}}{p_r} + \frac{16E_c e^{-2y}}{p_r} - \frac{8se^{-2y}}{p_r} + s^2e^{-y} - \frac{8Ne^{-2y}}{p_r} - N^2e^{-y} - 8E_c Ne^{-2y} + 4E_c L_1e^{-2y} - 4E_c e^{-2y} + E_c L_1\Omega e^{-y}\right)\frac{t^2}{2} \quad (40)$$

Thus,

$$\theta_3(y,t) = \mathcal{L}^{-1}\left\{\frac{1}{s}\left\{\frac{1}{p_r}\mathcal{L}[At^2] + s\mathcal{L}\left[\frac{Bt^2}{2}\right] + N\mathcal{L}\left[\frac{Ct^2}{2}\right] + E_c\mathcal{L}\left[\frac{Dt^2}{2}\right]\right\}\right\}$$

$$\theta_3(y,t) = \left(\frac{32e^{-2y}}{p_r^3} - \frac{2se^{-y}}{p_r^2} + \frac{2Ne^{-y}}{p_r^2} + \frac{32E_ce^{-2y}}{p_r^2} - \frac{16se^{-2y}}{p_r^2} + \frac{2s^2e^{-y}}{p_r} - \frac{16Ne^{-2y}}{p_r^2} - \frac{2N^2e^{-y}}{p_r} - \frac{16E_cNe^{-2y}}{p_r} + \frac{8E_cL_1e^{-2y}}{p_r} - \frac{8E_ce^{-2y}}{p_r} + \frac{2E_cL_1\Omega e^{-y}}{p_r} - \frac{16se^{-2y}}{p_r^2} + \frac{2s^2e^{-y}}{p_r} - \frac{2Nse^{-y}}{p_r} - \frac{16E_cse^{-2y}}{p_r} + \frac{2se^{-2y}}{p_r} - 2s^2e^{-y} + \frac{8Nse^{-2y}}{p_r} + 2N^2se^{-y} - 16E_cNse^{-2y} + 8E_csL_1e^{-2y} - 8E_cse^{-2y} + 2E_cL_1s\Omega e^{-y} + \frac{8Ne^{-2y}}{p_r^2} - \frac{2Nse^{-y}}{p_r} + \frac{2N^2e^{-y}}{p_r} + \frac{8E_cNe^{-2y}}{p_r} - \frac{4Nse^{-2y}}{p_r} + 2Ns^2e^{-y} - \frac{4N^2e^{-2y}}{p_r} - 2N^3e^{-y} - 4E_cN^2e^{-2y} + 2E_cNL_1e^{-2y} - 2E_cNe^{-2y} + 2E_cL_1N\Omega e^{-y} + 4E_cs^2e^{-2y} - 16E_cse^{-2y} + 16E_cL_1e^{-y} - 16E_cL_1e^{-2y} + 8E_cL_1se^{-2y} - 8E_ce^{-2y}\right)\frac{t^3}{3!} \quad (41)$$

Therefore, the solution to the temperature equation (7) is;

$$\theta(y,t) = \theta_0(y,t) + \theta_1(y,t) + \theta_2(y,t) + \theta_3(y,t) + \cdots$$

$$\theta(y,t) = e^{-y} + \left(\frac{e^{-2y}}{p_r} - se^{-y} + Ne^{-y} + E_ce^{-2y}\right)t + \left(\frac{4e^{-2y}}{p_r^2} - \frac{se^{-y}}{p_r} + \frac{Ne^{-y}}{p_r} + \frac{4E_ce^{-2y}}{p_r} - \frac{2se^{-y}}{p_r} + s^2e^{-y} - \frac{2Ne^{-2y}}{p_r} - N^2e^{-y} - 2E_cNe^{-2y} + E_cL_1e^{-2y} - E_ce^{-2y} + E_cL_1\Omega e^{-y}\right)\frac{t^2}{2!} + \left(\frac{32e^{-2y}}{p_r^3} - \frac{2se^{-y}}{p_r^2} + \frac{2Ne^{-y}}{p_r^2} + \frac{32E_ce^{-2y}}{p_r^2} - \frac{16se^{-2y}}{p_r^2} + \frac{2s^2e^{-y}}{p_r} - \frac{16Ne^{-2y}}{p_r^2} - \frac{2N^2e^{-y}}{p_r} - \frac{16E_cNe^{-2y}}{p_r} + \frac{8E_cL_1e^{-2y}}{p_r} - \frac{8E_ce^{-2y}}{p_r} + \frac{2E_cL_1\Omega e^{-y}}{p_r} - \frac{16se^{-2y}}{p_r^2} + \frac{2s^2e^{-y}}{p_r} - \frac{2Nse^{-y}}{p_r} - \frac{16E_cse^{-2y}}{p_r} + \frac{2se^{-2y}}{p_r} - 2s^2e^{-y} + \frac{8Nse^{-2y}}{p_r} + 2N^2se^{-y} - 16E_cNse^{-2y} + 8E_csL_1e^{-2y} - 8E_cse^{-2y} + 2E_cL_1s\Omega e^{-y} + \frac{8Ne^{-2y}}{p_r^2} - \frac{2Nse^{-y}}{p_r} + \frac{2N^2e^{-y}}{p_r} + \frac{8E_cNe^{-2y}}{p_r} - \frac{4Nse^{-2y}}{p_r} + 2Ns^2e^{-y} - \frac{4N^2e^{-2y}}{p_r} - 2N^3e^{-y} - 4E_cN^2e^{-2y} + 2E_cNL_1e^{-2y} - 2E_cNe^{-2y} + 2E_cL_1N\Omega e^{-y} + 4E_cs^2e^{-2y} - 16E_cse^{-2y} + 16E_cL_1e^{-y} - 16E_cL_1e^{-2y} + 8E_cL_1se^{-2y} - 8E_ce^{-2y}\right)\frac{t^3}{3!} \quad (42)$$

The physical momentum and heat properties such as the skin friction C_f and Nusselt number, which are elucidated in Joseph *et al*. (2021) are;

$$\begin{cases} C_f = -\frac{1}{2\sqrt{2}}G_r{}^{-3/4}\left(\frac{\partial u}{\partial y}\right)_{y=0} \\ N_u = -\frac{1}{2\sqrt{2}}G_r{}^{-3/4}\left(\frac{\partial \theta}{\partial y}\right)_{y=0} \end{cases} \quad (42)$$

RESULTS AND DISCUSSION

A turbulent boundary layer flow in the presence of constant pressure gradient, thermal radiation, and suction has been analysed. The effects of magnetic parameter M, suction parameter S, and pressure gradient Ω, on the velocity field were determined. Graphs for the different flow fields have been plotted. In the same view; the effects of thermal radiation N, Eckert number E_c, prandtl number P_r, and suction parameter S on temperaturere profile were also determined and graphs plotted.

The default values for the pertinent flow parameters are taken as Arifuzzaman *et al*., (2018)
$\Omega = 0.30$, $S = 0.30$, $P_r = 0.71$, $N = 0.05$, $Da = 1.00$, $t = 0.05$, $E_c = 1.00$

To validate the present work, a numerical comparison is provided in Table 1. It can be seen there is no significant difference. The impact of flow parameters on the skin friction C_f, and Nusselt number N_u is also investigated and presented in Table 2.

Table 1: Validation of present study against Joseph et al (2021) for the Nusselt number, where,
$Pr = 0.71$ and $Ec = 0$

N	Present Study	Joseph *et al* (2021)	Difference
1.00	0.00152	0.00167	0.00015
3.00	0.00144	0.00154	0.0001
5.00	0.00135	0.00151	0.00016
7.00	0.00132	0.00142	0.0001

Table 2. Computational values of the skin friction C_f and Nusselt number N_u

S	N	M	P_r	Ec	C_f	N_u
1.00	1.00	1.00	0.71	0.50	1.9580	0.0015
3.00					1.9203	0.0014
5.00	3.00				1.8841	0.0013
7.00	5.00				1.8492	0.0012
	7.00	3.00			1.7623	
		5.00			1.2562	
		7.00	0.11		0.3331	1.3187
			0.31			1.1135
			0.51	0.75		1.0450
				1.00		1.0503
				1.50		1.0609

Table 2 presents the effect of flow parameters on the skin friction C_f, and Nusselt number N_u. It is seen that the skin friction diminishes due to the increase in both magnetic and suction parameters. The Nusselt number increases with an increase in Eckert number Ec and Prandtl number P_r, and decreases with an increase in suction parameter S and radiation parameter.

Science World Journal Vol. 20(No 2) 2025 https://dx.doi.org/10.4314/swj.v20i2.32
www.scienceworldjournal.org
ISSN: 1597-6343 (Online), ISSN: 2756-391X (Print)
Published by Faculty of Science, Kaduna State University

Figure 2 illustrates the drag force effect on fluid flow. The velocity profile decreases with increment of magnetic parameter $M, (1.00 \leq M \geq 7.00)$. The role of magnetic parameter which is to suppress turbulence. Physically, when magnetic field is applied to any field, the apparent viscosity of the fluid increases to the point of becoming viscous elastic solid. It is of great interest that yields stress of the fluid can be controlled very accurately through variation of the magnetic field intesity. The result is that the ability of the fluid to transmit force can be controlled with help of electomagnet which give rise to many possible control-based applications,including MHD power generation, electromagnetic casting of metals, MHD propulsion etc.

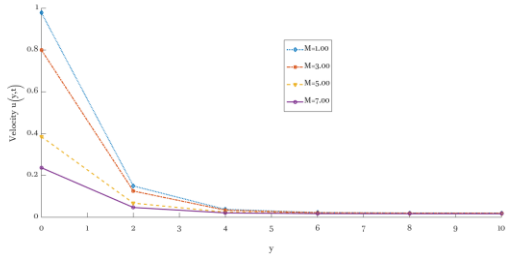

Figure 2: Influence of Magnetic Parameter M on Velocity

The flow is driven by an externally imposed pressure gradient without motion of either plate, negative or positive pressure gradient increase or decrease the flow rate, respectively. This is illustrated in Figure 3. It is seen that increase in pressure gradient Ω, enhance the flow significantly. Pressure gradient is physical quantity that describes which direction and at what rate the pressure changes the most rapidly around a particular location.

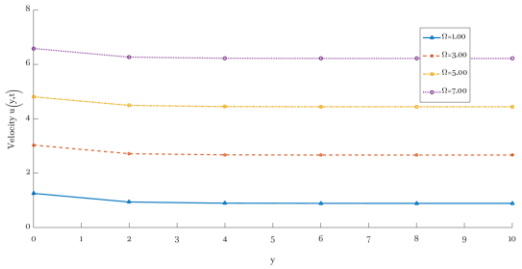

Figure 3: Influence of Pressure Gradient Ω on Velocity

The impact of the suction parameter S, on velocity and temperature profiles is illustrated in Figures 4 and 5 respectively. It is clearly seen that velocity and temperature profiles diminish with an increase of $S(1.00 \leq S \leq 7.00)$, this is due to porosity of plates.

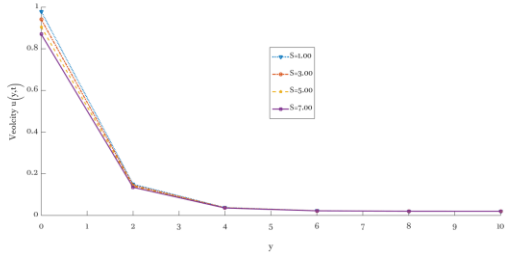

Figure 4: Influence of Suction Parameter S on Velocity

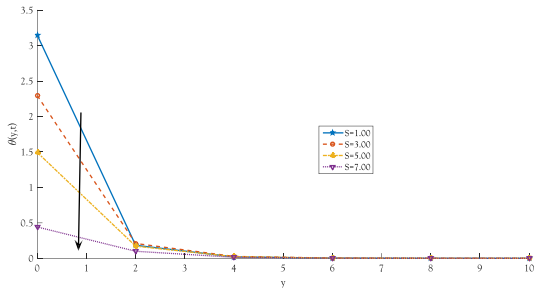

Figure 5: Influence of Suction Parameter S on Temperature

Figure 6 depicts the temperature field for increment of thermal radiation parameter N $(1.00 \leq N \geq 7.00)$. Thermal radiation is known as electromagnetic radiation or the conversion of thermal energy which generates thermal motion of particles in matter. Thermal radiation could be attributed due to thermal excitation. It is observed that the temperature field is affected significantly with increase in thermal radiation parameter N. Thermal radiation for a medium which contains it inevitably has pressure and density gradient, and the treatment requires the use of hydrodynamics.

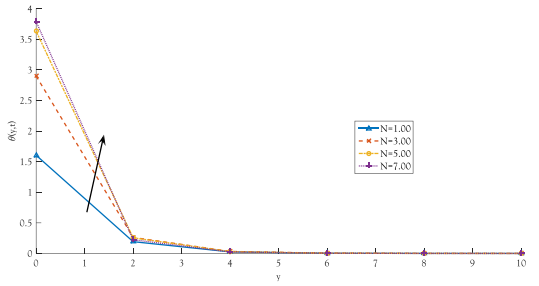

Figure 6: Influence of Thermal Radiation N on Temperature

Figure 7 shows the impression of Prandtl number, P_r, on temperature profile. The parameter, P_r, is the proportion of kinematic viscosity and thermal diffusivity which changes physically with temperature. For example, water, $P_r = 7.00\ (at\ 20°c)$ and Ammonia $P_r = 1.38$ decline more rapidly than air $P_r = 0.71$. However, increase in p_r depict the domination of thermal and diffusivity respectively. Prandtl number is used to determine whether heat transport occurs with either conduction or convection process. Since, Prandtl number is inversely proportional to thermal diffusivity so that increasing p_r led to the decrease in temperature profile.

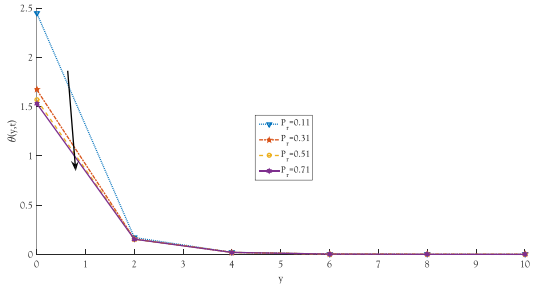

Figure 7: Influence of Prandtl Number P_r on Temperature

Figure 8 shows that an increase in Eckert number, E_c, from 0.50 through 0.75, 1.00 to 1.50 (very high viscous heating) clearly boosts temperature in the porous regime. Eckert number signifies the quantity of mechanical energy converted via internal friction to thermal energy. i.e. heat dissipation. Increasing E_c values will therefore cause an increase in thermal energy contributing to the flow and will heat the regime. For all nonzero values of E_c, the temperature overshoot near the wall is distinct, this overshoot migrates marginally further into the boundary layer with an increase in E_c.

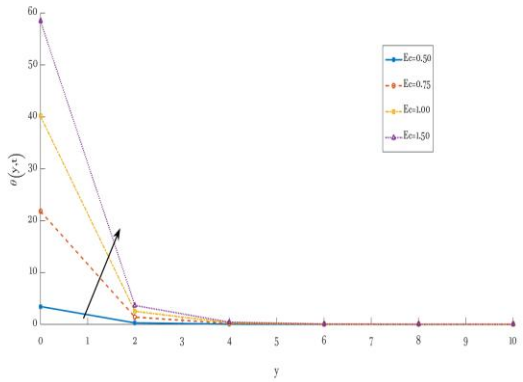

Figure 8: Influence of Eckert Number Ec on Temperature

CONCLUSION

This study investigated turbulent boundary layer flow under a constant pressure gradient and the influence of thermal radiation. The governing equations—the continuity, nonlinear momentum, and energy equations—were solved using the He-Laplace method, which combines the Homotopy Perturbation Method with the Laplace Transform technique. This approach yielded analytical expressions for velocity and temperature profiles.

The effects of fluid parameters, including the magnetic parameter (M), suction parameter (S) and pressure gradient (Ω) on velocity were analyzed and visualized through graphical representations. Similarly, the impact of thermal radiation parameter (N), Eckert number (Ec), Prandtl number (Pr), and suction parameter (S) on the temperature profile was examined and plotted.

Key findings include:

1. Temperature increases with higher thermal radiation parameter.
2. Velocity decreases with an increase in magnetic parameter.
3. A higher Prandtl number reduces the temperature profile.
4. Both velocity and temperature decrease with increasing suction parameter.
5. Velocity rises with an increase in pressure gradient.
6. The temperature profile is enhanced by a higher Eckert number.
7. Combined increases in magnetic and suction parameters reduce velocity.
8. The Nusselt number improves significantly with higher Eckert and Prandtl numbers.
9. Radiation and suction parameters lead to lower temperature distribution.

The results have practical applications in fields such as **automobile thermal systems**, magnetohydrodynamic (MHD) power generators, and various industrial processes including polymer dye extrusion and plastic film drainage.

Nomenclature

Ω	Pressure gradient
u, v	Dimensional velocity components of the fluid
x, y	Coordinate
θ	Dimensionless temperature of the fluid
σ	Stefan-Boltzmann Constant
ρ	Density of the fluid
μ	Dynamic viscosity of the fluid
ϑ	Kinematic viscosity of the fluid
p	Pressure of the fluid
S	Suction parameter
N	Radiation parameter
M	Magnetic parameter
L	Length of the plate
K	Coefficient of thermal conductivity
t	Dimensionless time
C_p	Specific temperature of the fluid under constant pressure
P_r	Prandlt number
E_c	Eckert number
T	Temperature of the fluid
T_0	Initial temperature of the fluid
T_w	Temperature of the flat plate
T_∞	Temperature of the fluid at the edge of the boundary layer
L_1	Auxilliary linear operator
$\mathcal{L}$	Auxilliary nonlinear operator
$\frac{\partial q_r}{\partial y}$	Local radiant absorption
q_r	Relative energy flux
δ	Dimensional boundary layer thickness
U_∞	Free stream velocity

REFERENCES

Arifuzzaman S. M. Shakhaoth Khan Md., Al-Mamum A., Reza-E-Rabbi S.K., Biswas P. and Karim I. (2018); *Hydrodynamic Stability and Heat and Mass Transfer Flow Analysis of MHD Radiative Fourth-Grade Fluid Through Porous Plate with Chemical Reaction*. Journal of King Saud University, 31 (4): 1388-1398.

Duan L., Martin M. P., Feldick A. M., Modest M. F and Levin D. A (2011). *Study of turbulence-radiation interaction in hypersonic turbulent boundary layers*. AIAA Journal. 50:447-453.

Duan L., Meelan M.C. and Zhang C. (2016). *Pressure fluctuations induced by a hypersonic turbulent boundary layer*, Journal of Fluid Mechanics, 804:578 – 607.

Dyke, M. V. (1975). *Perturbation method in fluid mechanics, parabolic press:* Stanford, CA, USA. Housiadas, K.D. and Tanner, R.I. (2016). *A high-order perturbation solution for the steady sedimentation of a sphere in a viscoelastic fluid.* J. Non-Newton. Fluid Mech. 233:166–180.

Housiadas, K.D., Ioannou, I. and Georgiou, G.C. (2018),

Lubrication solution of the axisymmetric Poiseuille flow of a Bingham fluid with pressure-dependent rheological parameters. J. Non-Newton. Fluid Mech. 260:76–86.

Housiadas, K.D. and Tanner, R.I. (2018), *Viscoelastic shear flow past an infinitely long and freely rotating cylinder*. Phys. Fluids 30:073101.

Hughes W. F and Brighton J. A (1991). *Fluid dynamics*, Schaun's outline series in engineering. McGraw-Hill book company.

Joseph, K. M., Ayankop-Andi, E. and Mohammed, S. U. (2021); *Unsteady MHD plane couette-poiseuille flow of fourthgrade fluid with thermal radiation, chemical reaction and suction effects*. Int. J. of Applied Mechanics and Engineering, 26(4): 77-98

Kafoussias N. and Xenos M. (2000). *Numerical study of two-dimensional turbulent boundary layer compressible flow with adverse pressure gradient and heat and mass transfer*. Acta Mech. 141:201-223.

Liao, S. J. (1992). *The proposed homtopy analysis techniques for the solution of nonlinear problems.* PhD thesis, Shanghai Jiao Tong University.

Liao, S.J. (1997), *A kind of approximate solution technique which does not depend upon small parameters-II.An application in fluid mechanics*, Int. J. Nonlin. Mech. 32:815–822.

Liao, S.J. (1999), An explicit totally analytic solution of laminar viscous flow over a semi-infinite flat plate. Commun. Nonlinear Sci. Numer. Simul. 3:53–57.

Liao, S.J. (2004), *Beyond Perturbation: Introduction to the Homotoy Analysis Method;* Chapman & Hall/CRC, CRC PressLLC: Boca Raton, FL, USA.

Liao, S.J. (2004). *On the homotopy analysis method for nonlinear problems*. Appl. Math. Comput. 147(2):499-513

Liao, S.J. (2011), *Homotopy Analysis Method in Nonlinear Differential Equations;* Springer: Berlin, Germany.

Mark P. Simens, Javier Jimenez, Sergio Hoyas and Yoshinori Mizuno (2009). *A high resolution code for turbulent boundary layers.* 228:4218-4231.

Muthucumaraswamy, R. (2006). *The interaction of thermal radiation on vertical oscillating plate with variable temperature and mass diffusion*. Theoretical and Applied Mechanics, 33:107-121.

Muthucumaraswamy, R. (2010), *Chemical Reaction Effects on Vertical Oscillating Plate with Variable Temperature*. Chemical Industry & Chemical Engineering Quarterly, 16(2):167−173.

Nargund A. L., Madhusudhan R. and Sathyanarayana S. B. (2017). *Study of compressible fluid flow in boundary layer region by homotopy analysis method*. Int. J. Latest Trend Eng. Technol. 9:28-39.

Rabenda, J. and Samarda, Z. (2015). *Convergence analysis of an iterative scheme for solving initial value problem for multidimensional partial differential equations*. Comp. Math. Appl. 70:1772-1780.

Rebenda J. and Smarda Z. (2016), *A semi-analytical approach for solving of nonlinear systems of functional differential equations with delay*, AIP Conference Proceedings 1863(1):530003

Rabenda, J. and Samarda, Z. (2019) *Numerical algorithm for nonlinear delayed differential systems of nth order*. Adv. Differ. Equ. 2019:26.

Reptis, A. and Perdikis, C. (2003). *Thermal radiation of an optically thin gray gas.* Int. J. Appl. Mech. Eng., 8:131-134.

Reptis, A. and Toki, C. J. (2009). *Thermal radiation in the presence of free convection flow past a moving vertical porous plate: An analytical solution*. Int. J. Appl. Mech. Eng., 14:1115-1126.

Sharma, R. P., Seshadri, R., Mishra, S. R., Munjam, S. R. (2019). *Effect of thermal radiation on magnetohydrodynamic three-dimension motion of a nanofluid past a shrinking surface under the influence of a heat source*. Heat Transfer-Asian Res. 48:2105-2121.

Xenos, M. (2013). *Radiation effects on flow past a stretching plate with temperature dependent viscosity.* Applied mathematics, 4:1-5.

Xenos M. (2017). *Thermal radiation effect on the MHD turbulent compressible boundary layer flow with adverse pressure gradient, heat transfer and local suction*. Open J. Fluid Dynamics. 7:1-14.

Xenos, M. and Pop, I. (2017) *Radiation Effect on the Turbulent Compressible Boundary Layer Flow with Adverse Pressure Gradient*. Applied Mathematics and Computation, 299:153-164.

Xenos, M., Eugenia N. P., Anastasios S. and U. S. Mahabaleshwar (2020). *Solving the nonlinear boundary layer flow equations with pressure gradient and radiation*. Helmholtz Centre for infection Research, Braunschweig, Germany, 12:710.